THE JOURNAL OF PHYSICAL CHEMISTRY C

Feature Article

New Non-Oxide Photocatalysts Designed for Overall Water Splitting under Visible Light

Kazuhiko Maeda, and Kazunari Domen

J. Phys. Chem. C, **2007**, 111 (22), 7851-7861• DOI: 10.1021/jp070911w • Publication Date (Web): 15 May 2007

FEATURE ARTICLE

New Non-Oxide Photocatalysts Designed for Overall Water Splitting under Visible Light

Kazuhiko Maeda and Kazunari Domen*

Department of Chemical System Engineering, University of Tokyo, 7-3-1 Hongo, Bunkyo-ku, Tokyo 113-8656, Japan

Received: February 1, 2007; In Final Form: March 15, 2007

Overall water splitting to form hydrogen and oxygen over a heterogeneous photocatalyst using solar energy is a promising process for clean and recyclable hydrogen production in large-scale. In recent years, numerous attempts have been made for the development of photocatalysts that work under visible-light irradiation to efficiently utilize solar energy. This article presents recent research progress in the development of visible-light-driven photocatalysts, focusing on the refinement of non-oxide-type photocatalysts such as (oxy)nitrides and oxysulfides.

1. Introduction

To effectively address the depletion of fossil fuels and the serious environmental problems accompanying their combustion, modern society has been searching for a new form of energy that is clean, renewable, cheap, and a viable alternative to fossil fuels. Recently, much attention has been paid to hydrogen as a next-generation energy carrier, and over the past 3 decades, photocatalytic overall water splitting using solar energy has been studied as a potential method of hydrogen production. Research on such catalysts was triggered by the work of Honda and Fujishima, who demonstrated that overall water splitting can be achieved using a photoelectrochemical (PEC) cell consisting of a single-crystalline TiO_2 (rutile) anode and a Pt cathode under ultraviolet (UV) irradiation and an external bias.[1] Since then, a large number of PEC cells have been developed, many of which are designed specifically for the efficient utilization of solar energy. However, due to the lack of suitable photoelectrode materials with appropriate band gap structures and stability, the systems proposed to date have been rather complicated, integrated multilayer and tandem systems being examples.[2−4] Overall water splitting for the production of hydrogen using a particulate photocatalyst, similar in many ways to the photosynthetic reaction, have also been examined since 1980.[5−7] From the viewpoint of large-scale hydrogen production, particulate photocatalyst systems are considered to be advantageous over more complex multilayer or tandem structure devices and have a wider range of potential applications,[8] although a method for separating the simultaneously produced H_2 and O_2 remains to be developed.

Thermodynamically, the overall water splitting reaction is an uphill reaction with a large positive change in Gibbs free energy ($\Delta G° = 238$ kJ/mol). Figure 1 shows a schematic illustration of the basic principle of overall water splitting on a heterogeneous photocatalyst. Under irradiation at an energy equivalent to or greater than the band gap of the semiconductor photocatalyst, electrons in the valence band are excited into the conduction band, leaving holes in the valence band. These photogenerated electrons and holes cause reduction and oxidation reactions, respectively. To achieve overall water splitting, the bottoms of the conduction bands must be located at a more negative potential than the reduction potential of H^+ to H_2 (0 V vs NHE at pH 0), while the tops of the valence bands must be positioned more positively than the oxidation potential of H_2O to O_2 (1.23 V vs NHE). Therefore, the minimum photon energy thermodynamically required to drive the reaction is 1.23 eV, corresponding to a wavelength of ca. 1000 nm, in the near-infrared region. Accordingly, it would appear to be possible to utilize the entire spectral range of visible light. However, there is an activation barrier in the charge-transfer process between photocatalysts and water molecules, necessitating a photon energy greater than the band gap of the photocatalyst to drive the overall water splitting reaction at reasonable reaction rates. In addition, the backward reaction, that is, water formation from H_2 and O_2, must be strictly inhibited, and the photocatalysts themselves must be stable in the reaction. Furthermore, although there are a large number of materials that possess suitable band gap potentials, there are very few materials that function as a

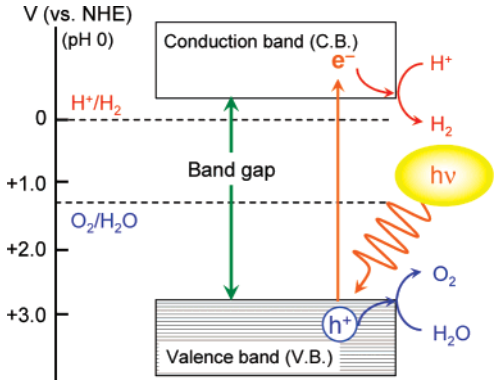

Figure 1. Basic principle of overall water splitting on a heterogeneous photocatalyst.

* To whom correspondence should be addressed. E-mail: domen@chemsys.t.u-tokyo.ac.jp. Tel: +81-3-5841-1148. Fax: +81-3-5841-8838.

10.1021/jp070911w CCC: $37.00
Published on Web 05/15/2007

Kazuhiko Maeda received a B.S.c. in chemistry from the Tokyo University of Science in 2003 and a M.S.c. in chemistry from the Tokyo Institute of Technology in 2005. He is currently a Ph.D. candidate in chemical systems engineering at The University of Tokyo under the supervision of Professor Kazunari Domen. His research interests include the development of new classes of materials, such as particulate semiconductors and nanoparticles, and the application of such materials as photocatalysts for overall water splitting.

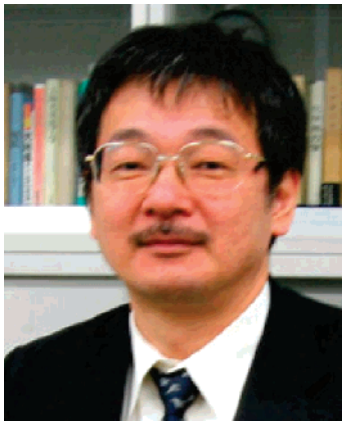

Kazunari Domen received B.S.c. (1976), M.S.c. (1979), and Ph.D. (1982) honors in chemistry from the University of Tokyo. He joined the Tokyo Institute of Technology in 1982 as Assistant Professor and was subsequently promoted to Associate Professor in 1990 and Professor in 1996. Moving to the University of Tokyo in 2004, his research interests now include heterogeneous catalysis and materials chemistry, with particular focus on surface chemical reaction dynamics, photocatalysis, solid-acid catalysis, and mesoporous materials. Further information on the Domen research group can be found at http://www.domen.t.u-tokyo.ac.jp/.

photocatalyst for overall water splitting due to other factors, as mentioned below.

As shown in Figure 2, the overall water splitting reaction on a semiconductor photocatalyst occurs in three steps, (1) the photocatalyst absorbs photon energy greater than the band gap energy of the material and generates photoexcited electron−hole pairs in the bulk, (2) the photoexcited carriers separate and migrate to the surface without recombination, and (3) adsorbed species are reduced and oxidized by the photogenerated electrons and holes to produce H_2 and O_2, respectively. The first two steps are strongly dependent on the structural and electronic properties of the photocatalyst. In general, high crystallinity has a positive effect on activity since the density of defects, which act as recombination centers between photogenerated carriers, decreases with increasing crystallinity. The third step, on the other hand, is promoted by the presence of a solid cocatalyst. The cocatalyst is typically a noble metal (e.g., Pt, Rh) or metal oxide (e.g., NiO, RuO_2) and is loaded onto the photocatalyst surface as a dispersion of nanoparticles to produce active sites

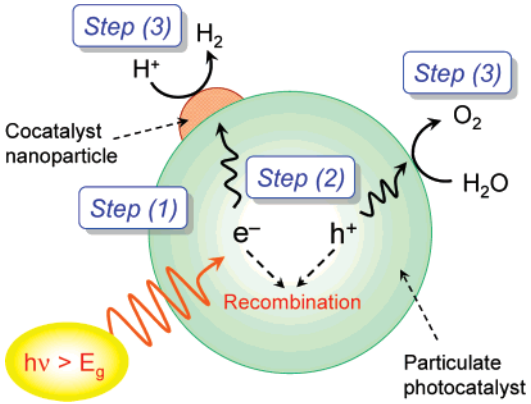

Figure 2. Processes involved in photocatalytic overall water splitting on a heterogeneous photocatalyst.

TABLE 1: Representative Metal Oxide Photocatalysts with d^0 or d^{10} Electronic Configuration[a]

d^0-Type Photocatalysts	
element	photocatalyst
Ti^{4+}	TiO_2,[6] $SrTiO_3$,[5,7,9] $Na_2Ti_6O_{13}$,[12] $BaTi_4O_9$,[13] $K_2La_2Ti_3O_{10}$[14,15]
Zr^{4+}	ZrO_2[23]
Nb^{5+}	$K_4Nb_6O_{17}$,[10,11] $Sr_2Nb_2O_7$[17]
Ta^{5+}	$K_3Ta_3Si_2O_{13}$,[16] $ATaO_3$ (A = Li, Na, K),[18,20] $NaTaO_3$:La,[22] $BaTa_2O_6$,[18] $RbNdTa_2O_7$,[19] $H_2SrTa_2O_7 \cdot nH_2O$[21]
W^{6+}	$AMWO_6$ (A = Rb, Cs; M = Nb, Ta)[24]
d^{10}-Type Photocatalysts	
element	photocatalyst
Ga^{3+}	$ZnGa_2O_4$[26]
In^{3+}	$AInO_2$ (A = Li, Na),[28] AIn_2O_4 (A = Ca, Sr)[25,29]
Ge^{4+}	Zn_2GeO_4[30]
Sn^{4+}	Sr_2SnO_4[25]
Sb^{5+}	$NaSbO_3$,[25,27] $CaSb_2O_6$,[27] $A_2Sb_2O_7$ (A = Ca, Sr)[27]

[a] Superscripts denote cited references.

and reduce the activation energy for gas evolution. It is thus important to design both the bulk and surface properties of the material carefully so as to obtain high photocatalytic activity for this reaction.

Until the middle of the 1980s, research on particulate photocatalysts for overall water splitting had largely been devoted to $SrTiO_3$ and TiO_2.[5−7,9] Since the discovery of $K_4Nb_6O_{17}$, which has a layered structure and high photocatalytic activity,[10,11] photocatalysts having unique structures, such as layered, tunnel, and pillared structures, have also been reported.[12−17] Since the second half of the 1990s, many tantalates have been reported to be highly active photocatalysts.[16,18−22] ZrO_2 has also been reported to be a unique photocatalyst, exhibiting high activity even without a cocatalyst.[23] Recently, tungsten-based metal oxides, $AMWO_6$ (A = Rb, Cs; M = Nb, Ta), have been found to be active under UV for the stoichiometric cleavage of water.[24] Inoue et al. also reported typical metal oxides with d^{10} electronic configuration as a new class of photocatalysts suitable for overall water splitting.[25−30] Figure 3 shows the groups of metallic elements that can form suitable band gap structures of the corresponding oxide materials and which have been successfully applied as photocatalysts for overall water splitting. In all cases, the oxidation states of the metallic elements in such photocatalysts are the highest, that is, Ti^{4+}, Zr^{4+}, Nb^{5+}, Ta^{5+} and W^{6+}, in the red group and Ga^{3+},

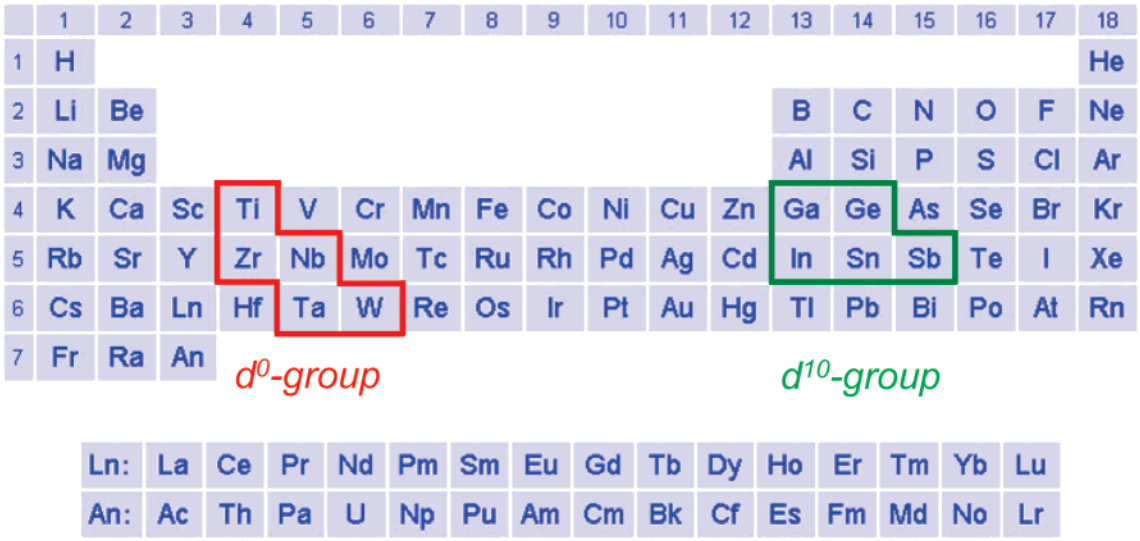

Figure 3. Principal cation components for photocatalytic overall water splitting.

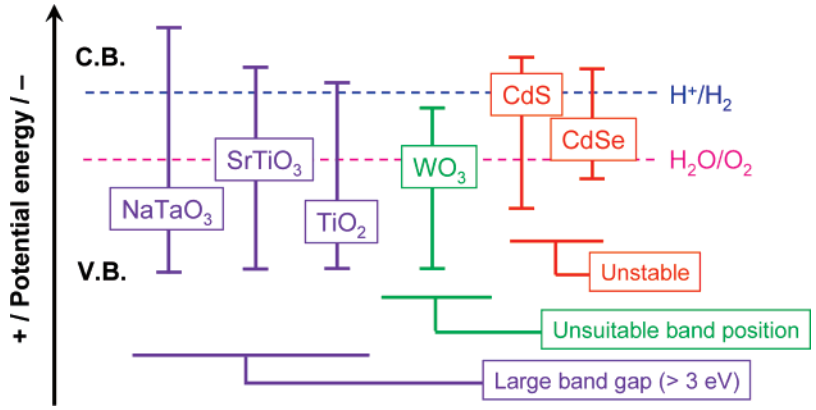

Figure 4. Schematic illustration of band structures of several semiconductor photocatalysts.

In^{3+}, Ge^{4+}, Sn^{4+}, and Sb^{5+} in the green group (as indicated in the figure). Photocatalysts based on transition-metal cations with empty d orbitals are defined as having a d^0 electronic configuration (red group), while those based on typical metal cations with filled d orbitals are defined as having a d^{10} electronic configuration (green group). Representative photocatalysts with these d^0 or d^{10} electronic configurations are listed in Table 1. Other metal oxides with d^0 or d^{10} electronic configurations, such as V^{5+}, Mo^{6+}, and Zn^{2+}, are also expected to be active as photocatalysts for overall water splitting, although there are, as of yet, no reports on such photocatalysts with reasonable activity. A number of metal oxide photocatalysts have been proposed to date, and some have achieved high quantum efficiencies as high as 30−50%.[15,22] However, the tops of the valence bands of such metal oxide photocatalysts, having d^0 or d^{10} metal cations, usually consist of O2p orbitals, which are located at ca. +3 V or higher (vs NHE). Therefore, if the bottom of the conduction band of a given metal oxide is located at a potential more negative than the water reduction potential, the band gap of the material will inevitably becomes larger than 3 eV, rendering the material inactive in the visible-light region.[31]

2. Strategy for Development of Visible-Light-Driven Photocatalysts

From the viewpoint of solar energy utilization, the development of a photocatalyst that splits water efficiently under visible light (λ > 400 nm) is indispensable. Until the first half of the 1990s, only a few chalcogenides and metal oxides (e.g., CdS and WO_3)[32−36] were known to be photocatalytically active under visible light. Certain metal chalcogenides, including CdS and CdSe, appear to be suitable photocatalysts for overall water splitting, exhibiting band gap energies sufficiently small to allow absorption of visible light and having conduction and valence bands at potentials appropriate for water reduction and oxidation. These metal chalcogenides, however, are not stable in the water oxidation reaction to form O_2 because the S^{2-} and Se^{2-} anions are more susceptible to oxidation than water, causing the CdS or CdSe catalyst itself to be oxidized and degraded.[37,38] Although WO_3 functions as a stable photocatalyst for O_2 evolution under visible light in the presence of an appropriate electron acceptor, the bottom of the conduction band of the material is located at a more positive potential than the potential of water reduction. As a result, WO_3 does not have the ability to reduce H^+ to H_2. Figure 4 depicts a schematic illustration of band structures of some photocatalysts, which presents the above-mentioned dilemma. Until very recently, reproducible photocatalytic systems for visible-light-driven overall water splitting had not been realized, although there are several reports that claimed to demonstrate the decomposition of water under visible light. Therefore, overall water splitting by visible light had been once described as one of the "Holy Grails" of chemistry.[8]

The difficulty in developing a suitable photocatalyst can be attributed to the lack of known materials that meet all three requirements, (1) band edge potentials suitable for overall water splitting, (2) band gap energy smaller than 3 eV, and (3) stability in the photocatalytic reaction. To date, numerous attempts have

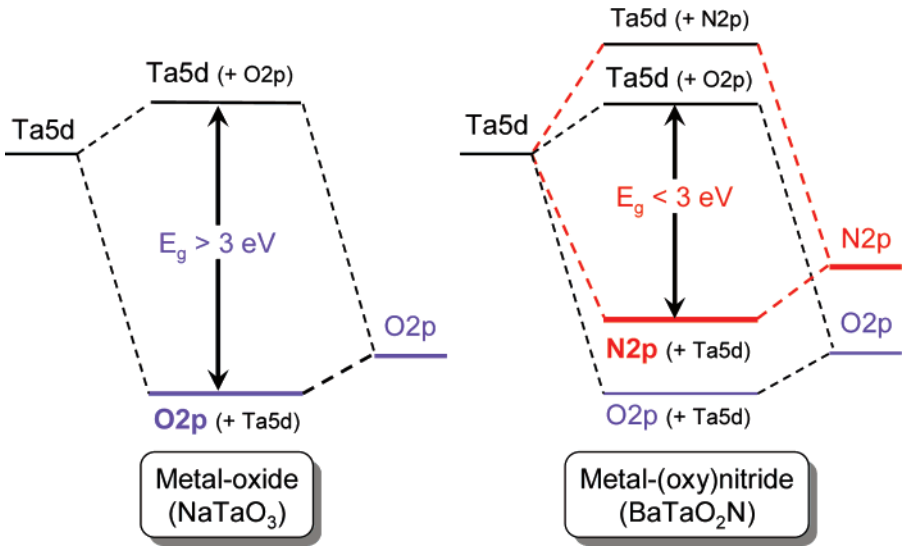

Figure 5. Schematic band structures of a metal oxide ($NaTaO_3$) and metal (oxy)nitride ($BaTaO_2N$).

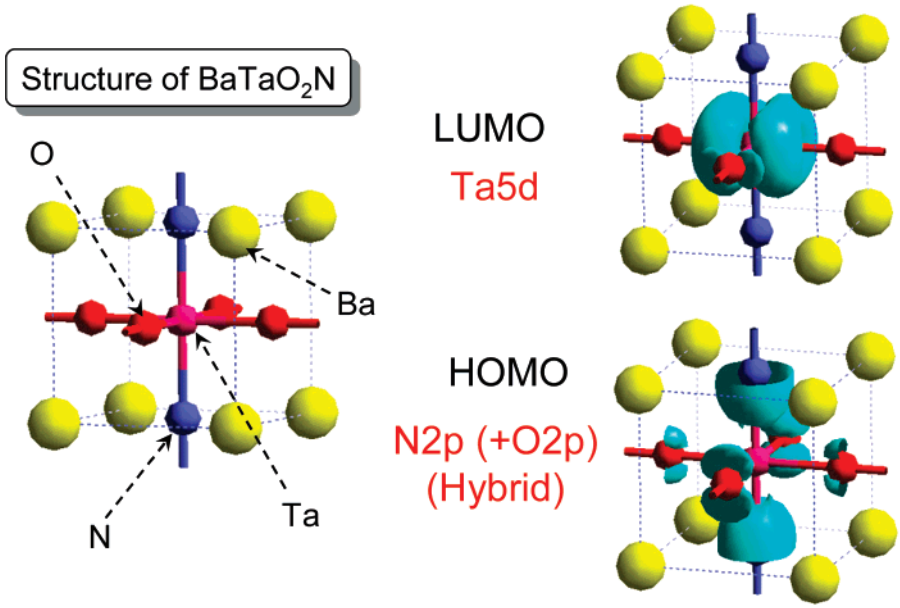

Figure 6. Band structure of $BaTaO_2N$ by DFT calculations.

been made to prepare a photocatalytic material that efficiently works under visible light.[39−52] In the development of such a photocatalyst, it is primarily important to control the band structure. In UV-active metal oxide photocatalysts, the bottoms of the conduction bands, which consist mainly of empty transition-metal d orbitals, are located at a potential slightly more negative than 0 V (vs NHE) at pH 0, and the tops of the valence bands, consisting of O2p atomic orbitals, are more positive than 3 V.[31] As mentioned above, this situation causes a band gap of the material too large to harvest visible light, nevertheless suggesting that metal oxide photocatalysts have enough potential to oxidize water, judging from the difference between the oxidation potential of H_2O into O_2 (1.23 V vs NHE) and the valence band edge potential (ca. 3 V vs NHE). Therefore, when other elements (e.g., N2p and S3p) having atomic orbitals with a potential energy higher than O2p atomic orbitals are introduced into a metal oxide, new valence bands can be formed instead of pure O2p atomic orbitals, which results in decreasing the band gap energy without affecting the conduction band level, thus producing a visible-light-driven photocatalyst with band edge potentials suitable for overall water splitting.

The authors' group has studied such materials, in particular (oxy)nitrides and oxysulfides, as photocatalysts for overall water splitting under visible light. Note that this type of material differs from materials doped with nitrogen or sulfur.[53] Figure 5 shows the schematic band structures of the metal oxide $NaTaO_3$ and (oxy)nitride $BaTaO_2N$, both of which have the same perovskite structure. The top of the valence band (i.e., highest occupied molecular orbital, HOMO) for the metal oxide consists of O2p orbitals. When N atoms are partially or fully substituted for O atoms in a metal oxide, the HOMO of the material is expected to be shifted higher compared to the corresponding metal oxide, without affecting the level of the bottom of the conduction band (i.e., lowest unoccupied molecular orbital, LUMO). The band structure of $BaTaO_2N$ obtained by density functional theory (DFT) calculations is shown in Figure 6. As expected, the HOMO consists of hybridized N2p and O2p orbitals, whereas the LUMO is mainly composed of empty Ta5d orbitals. The potential of the HOMO for the (oxy)nitride is located at a higher potential energy than that for the corresponding oxide due to the contribution of N2p orbitals, making the band gap energy

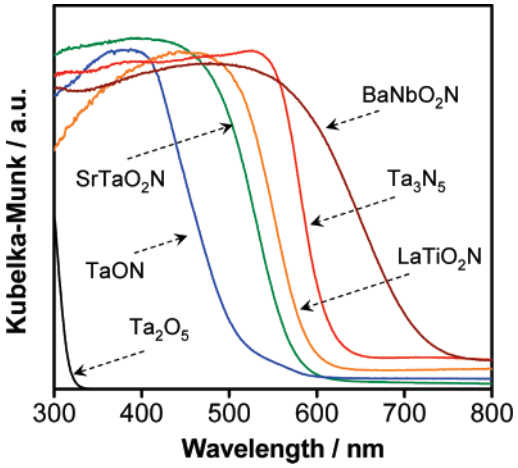

Figure 7. UV−visible diffuse reflectance spectra for (oxy)nitrides containing Ti^{4+}, Nb^{5+}, and Ta^{5+}.

sufficiently small to respond to visible light (<3 eV). A similar result was obtained in calculations for oxysulfides.

The doping of foreign elements into UV-active metal oxides is a conventional method employed for the preparation of visible-light-responsive photocatalysts.[44,47,50] In such doped photocatalysts, however, dopants in the photocatalyst act not only as visible-light absorption centers, with an absorption coefficient dependent on the density of dopants, but also as recombination sites between photogenerated electrons and holes. Furthermore, the impurity levels created by dopants in the forbidden band of the material are usually discrete, which would appear disadvantageous for the migration of photogenerated holes. In contrast, (oxy)nitrides and oxysulfides contain N or S as constituent elements that form the tops of the valence band. Thus, photogenerated holes can migrate smoothly in the valence band of the material, which is particularly advantageous for water oxidation involving 4-electron transfer.

By a similar strategy, metal oxides based on Pb^{2+},[39,48] Bi^{3+},[41,42] Ag^{+},[45] or Sn^{2+},[46] exhibiting visible-light photocatalytic activity due to the presence of s electrons of such elements, have also been developed. Although overall water splitting has yet to be achieved using these metal oxide photocatalysts, some have been successfully applied to the Z-scheme water splitting system mimicking natural photosynthesis in green plants, which involves two-step photoexcitation.[43,49,52]

3. (Oxy)nitrides with d^0 Electronic Configuration

Some particulate (oxy)nitrides containing early-transition-metal cations are stable and harmless materials and can be readily obtained by nitriding a corresponding metal oxide powder.[54−62] Figure 7 shows the UV−visible diffuse reflectance spectra for certain (oxy)nitrides containing transition-metal cations of Ti^{4+}, Nb^{5+}, and Ta^{5+} with d^0 electronic configuration. It is apparent that these (oxy)nitrides possess absorption bands at 500−750 nm, corresponding to band gap energies of 1.7−2.5 eV. As expected from DFT calculations, these (oxy)nitrides have band edge potentials suitable for overall water splitting, as revealed by UV photoelectron spectroscopy (UPS) and photoelectrochemical (PEC) analysis.[63] The band structures of Ta_2O_5, TaON, and Ta_3N_5 determined by UPS and PEC analysis are depicted schematically in Figure 8. It is clear that the tops of the valence bands are shifted to higher potential energies in the order Ta_2O_5 < TaON < Ta_3N_5, whereas the potentials of the bottoms of the conduction bands are almost the same. Investigation of the nitridation process for the preparation of

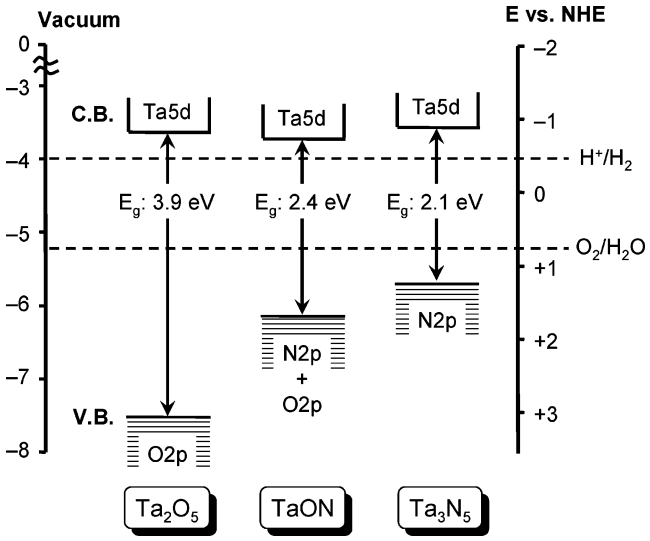

Figure 8. Schematic illustration of band structures of Ta_2O_5, TaON, and Ta_3N_5.

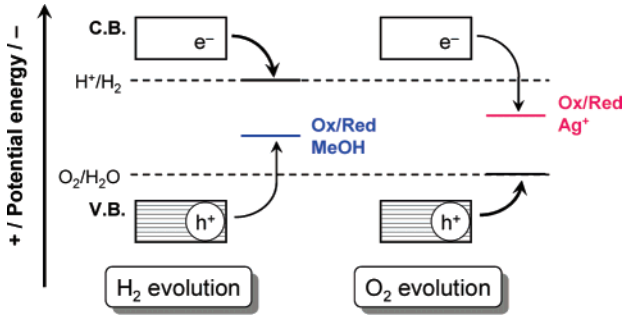

Figure 9. Basic principle of photocatalytic reactions in the presence of sacrificial reagents.

TaON and Ta_3N_5 from Ta_2O_5 by X-ray diffraction (XRD) measurements and high-resolution transmission electron microscopy (HR-TEM) have revealed that the solid-state transformation of Ta_2O_5 reacted with NH_3 to TaON and Ta_3N_5 is pseudomorphic and topotactic, producing single-crystalline particles of TaON and Ta_3N_5 with a porous structure from the single-crystalline Ta_2O_5 particle precursor.[64]

As overall water splitting is generally difficult to achieve due to the uphill nature of the reaction, photocatalytic activities of a number of (oxy)nitrides for water reduction or oxidation were examined in the presence of methanol or silver nitrate as a sacrificial reagent. The reactions using sacrificial reagents are not "overall" water splitting reactions but are often carried out as test reactions for overall water splitting.[39−52] The basic principle of photocatalytic reactions using sacrificial reagents is depicted schematically in Figure 9. When the photocatalytic reaction is conducted in the presence of an electron donor such as methanol, photogenerated holes in the valence band irreversibly oxidize methanol instead of H_2O, thus facilitating water reduction by conduction band electrons if the bottom of the conduction band of the photocatalyst is located at a more negative potential than the water reduction potential. On the other hand, in the presence of an electron acceptor such as silver cations, photogenerated electrons in the conduction band irreversibly reduce electron acceptors instead of H^+, thereby promoting water oxidation by valence band holes if the top of the valence band of the photocatalyst is positioned at a more positive level than the water oxidation potential.

Table 2 lists the photocatalytic activities of d^0 (oxy)nitrides for H_2 or O_2 evolution in the presence of sacrificial reagents.

TABLE 2: Photocatalytic Activities of (Oxy)nitrides with d^0 Electronic Configuration for H_2 or O_2 Evolution in the Presence of Sacrificial Reagents under Visible Light (λ > 420 nm)[a]

photocatalyst	band gap energy[b] eV	activity μmol h^{-1} H_2[c]	activity μmol h^{-1} O_2[d]	ref
$LaTiO_2N$	2.0	30	41	58
$Ca_{0.25}La_{0.75}TiO_{2.25}N_{0.75}$	2.0	5.5	60	58
$CaNbO_2N$	1.9	1.5	46	57
TaON	2.5	20	660	55
Ta_3N_5	2.1	10	420	56
$CaTaO_2N$	2.4	15	0	62
$SrTaO_2N$	2.1	20	0	62
$BaTaO_2N$	1.9	15	0	62
$LaTaO_2N$	2.0	20	0	57

[a] Reaction conditions: 0.2−0.4 g of catalyst, 200 mL of aqueous solution containing sacrificial reagents, 300 W xenon lamp light source, Pyrex top irradiation-type reaction vessel with cutoff filter. [b] Estimated from onset wavelength of diffuse reflectance spectra. [c] Loaded with nanoparticulate Pt as a cocatalyst; reacted in the presence of methanol (10 vol %) sacrificial reagent. [d] Sacrificial reagent: silver nitrate (0.01 M).

These (oxy)nitrides exhibit relatively high photocatalytic activity for water oxidation to form molecular oxygen under visible irradiation (λ > 420 nm), with some exceptions, such as $ATaO_2N$ (A = Ca, Sr, Ba) and $LaTaON_2$. Among this group, TaON achieves the highest quantum efficiency of 34%.[55] It should be noted that water oxidation involving a 4-electron process can be achieved by (oxy)nitrides with high quantum efficiencies, although silver nitrate is used as an electron accepter in such a system. In contrast, nitrogen-doped TiO_2 displays negligible activity for this reaction under the same reaction conditions.[60] (Oxy)nitrides also produce H_2 from an aqueous methanol solution upon visible irradiation when loaded with nanoparticulate Pt as a cocatalyst for H_2 evolution. However, the activities for H_2 production are about an order of magnitude lower than those for O_2 evolution, although the photocatalytic performance for H_2 evolution is stable. In this context, several new modifications to enhance the H_2 evolution rate of (oxy)-nitrides have been pursued, and it has been found that the photocatalytic activity of TaON for water reduction can be increased markedly by the photodeposition of Ru nanoparticles as H_2 evolution sites.[65] High-pressure treatment of Ta_3N_5 with NH_3 gas is also effective for enhancing the H_2 evolution activity.[66]

In most cases, a low level of N_2 evolution accompanies the initial stage of photocatalytic reactions over these catalysts, indicating that the (oxy)nitride is partially decomposed by the photogenerated holes (instead of water oxidation) according to the reaction

$$2N^{3-} + 6h^+ \rightarrow N_2$$

However, the production of N_2 is completely suppressed as the reaction progresses, and no change in the XRD pattern of the (oxy)nitrides as a result of the reaction has been detected. It thus appears that (oxy)nitride photocatalysts are essentially stable in the individual water reduction and oxidation reactions. It then remains to extend this performance to overall water splitting, which has yet to be achieved. The main obstacle appears to be the low activity of H_2 evolution on (oxy)nitrides. As these (oxy)-nitrides are typically synthesized by nitriding a corresponding oxide precursor under a flow of NH_3 at temperatures higher than 1073 K, it is considered that the (oxy)nitride is decomposed

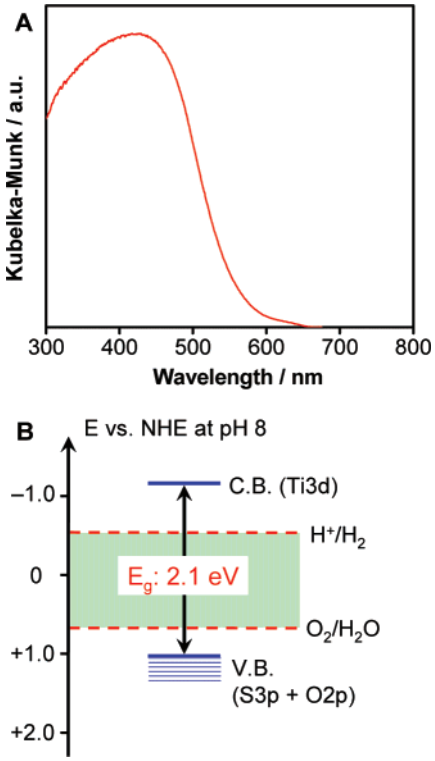

Figure 10. (A) UV−visible diffuse reflectance spectrum and (B) schematic illustration of band edge potentials of $Sm_2Ti_2S_2O_5$.

at the high temperature of nitridation, introducing nitrogen vacancies in the crystalline product. Nitrogen vacancies produce large band bending at the solid−liquid interface, forming a Schottky-type barrier[67] that hinders the prompt migration of electrons from the bulk to the surface reaction sites. Improvement of the preparation method to reduce the defect density in the d^0-type (oxy)nitride photocatalysts is, therefore, considered to be one of the key routes for further refinement. Nevertheless, Z-scheme overall water splitting under visible light has been achieved using a Pt-loaded TaON catalyst for H_2 evolution and a Pt-loaded WO_3 catalyst for O_2 evolution in the presence of an IO_3^-/I^- shuttle redox mediator.[68]

4. Oxysulfide, $Ln_2Ti_2S_2O_5$ (Ln: Pr, Nd, Sm, Gd, Tb, Dy, Ho, and Er)

The oxysulfide $Sm_2Ti_2S_2O_5$ is a stable photocatalyst with a wide absorption band in the visible region (λ < 600 nm) and band edge potentials suitable for overall water splitting, as shown in Figure 10.[69] This material can be obtained by heating a mixture of the corresponding precursors under vacuum and also by sulfurization of the corresponding metal oxide powder using H_2S gas.[70] DFT calculations indicate that the S3p atomic orbitals constitute the upper part of the valence band of $Sm_2Ti_2S_2O_5$ and make an essential contribution to lowering the band gap energy from that of the corresponding metal oxide ($Sm_2Ti_2O_7$). Metal sulfides such as CdS are not suitable for use as a photocatalyst for water oxidation due to the inherent instability of these materials in the reaction via the photogeneration of holes.[37,38] Interestingly, $Sm_2Ti_2S_2O_5$ functions as a stable photocatalyst for water oxidation to produce O_2. Deposition of colloidal IrO_2 nanoparticles as a water oxidation promoter[72,73] onto the $Sm_2Ti_2S_2O_5$ increases the quantum efficiency for O_2 evolution to 1.1%. It has also been confirmed by XRD and X-ray photoelectron spectroscopy (XPS) that decomposition of $Sm_2Ti_2S_2O_5$ in the bulk and at the surface, in particular the

oxidation of S^{2-} species, does not occur during water photooxidation, even though the valence band partially consists of S3p atomic orbitals. $Sm_2Ti_2S_2O_5$ has a Ruddlesden−Popper layered perovskite structure in which the layers are composed of S−(TiO_2)−O−(TiO_2)−S double octahedra. The formation of $TiSO_5$ octahedra results in the hybridization of S3p and O2p atomic orbitals constituting the valence band. It is likely that the hybridized S3p and O2p atomic orbitals are more stable than pure S3p atomic orbitals. H_2 evolution from an aqueous solution containing S^{2-} and SO_3^{2-} also proceeds steadily on $Sm_2Ti_2S_2O_5$ when modified with nanoparticulate Pt as H_2 evolution sites. On the basis of these results, it is concluded that the oxysulfide $Sm_2Ti_2S_2O_5$ has functionality as a stable photocatalyst for water reduction or oxidation under visible irradiation. Other $Ln_2Ti_2S_2O_5$ (Ln: Pr, Nd, Gd, Tb, Dy, Ho, and Er) oxysulfides with the same layered perovskite structure are also active and stable photocatalysts for H_2 or O_2 evolution from an aqueous solution containing a sacrificial electron donor or acceptor under visible irradiation.[71] The photocatalytic activities of $Ln_2Ti_2S_2O_5$ are dependent strongly on the kind of lanthanoid (Ln), which affects the electronic band structure.

5. (Oxy)nitrides with d^{10} Electronic Configuration

5.1. Difference in Electronic Band Structure between d^0- and d^{10}-Based Photocatalysts. The (oxy)nitride and oxysulfide photocatalysts having the ability to reduce and/or oxidize water under visible light are composed of transition-metal cations of Ti^{4+}, Nb^{5+}, or Ta^{5+} with d^0 electronic configuration.[55−71] From the viewpoint of the electronic band structure, however, d^{10}-based semiconducting materials are advantageous over the d^0 configurations as a photocatalyst in that, while the top of the valence band consists of O2p orbitals, the bottom of the conduction band is composed of hybridized s,p orbitals of typical metals.[25−30] The hybridized s,p orbitals possess large dispersion, leading to increased mobility of photogenerated electrons in the conduction band and thus high photocatalytic activity.[25−30] This has stimulated study on (oxy)nitrides or oxysulfides with the d^{10} electronic configuration as a photocatalyst for overall water splitting.

5.2. β-Ge_3N_4. As a typical metal nitride with d^{10} electronic configuration, β-Ge_3N_4 is synthesized from GeO_2 powder by nitridation under a flow of NH_3 at 1153−1173 K for 10 h.[74−76] The photocatalytic activity of the as-synthesized β-Ge_3N_4 for overall water splitting is negligible. However, when modified with RuO_2 nanoparticles, the material becomes photocatalytically active for the stoichiometric evolution of H_2 and O_2 from pure water. This demonstration of the photodecomposition of water is the first involving a non-oxide photocatalyst. High-pressure treatment of β-Ge_3N_4 with NH_3 gas was found to produce a 4-fold increase in activity by reducing the density of defects.[75] The photocatalytic performance of RuO_2-loaded β-Ge_3N_4 is strongly dependent on the pH of the aqueous solution, with the activity increasing with decreasing pH from pH 7, passing through a maximum at pH 0, and then decreasing.[76] This characteristic pH dependence of the RuO_2-loaded β-Ge_3N_4 photocatalyst deviates significantly from the general character of transition-metal oxide-based photocatalysts. For example, NiO_x-loaded $SrTiO_3$[9] and NiO-loaded $NaTaO_3$[20] photocatalysts favor neutral or alkaline solutions for overall water splitting.

The electronic band structure of β-Ge_3N_4 was examined by DFT calculations, which revealed that the tops of the valence band are formed by N2p orbitals, whereas the bottoms of the conduction band consist of hybridized 4s,4p orbitals of Ge. This result indicates that the photoexcitation under irradiation occurs from the N2p orbitals to the Ge4s,4p hybridized orbitals. Water oxidation to produce O_2 on conventional metal oxide photocatalysts takes place as a result of contributions from photogenerated holes in the valence band consisting of O2p orbitals. It is noteworthy that the N2p orbitals in the valence band both generate photogenerated holes and contribute to the photocatalytic water oxidation in the overall water splitting reaction. Unfortunately, β-Ge_3N_4 has a band gap of ca. 3.8 eV and is thus only active under UV irradiation. Nevertheless, the discovery of such a non-oxide photocatalyst (β-Ge_3N_4) achieving the same function as metal oxide photocatalysts provides strong encouragement for research on non-oxide materials for visible-light-driven photocatalysis.

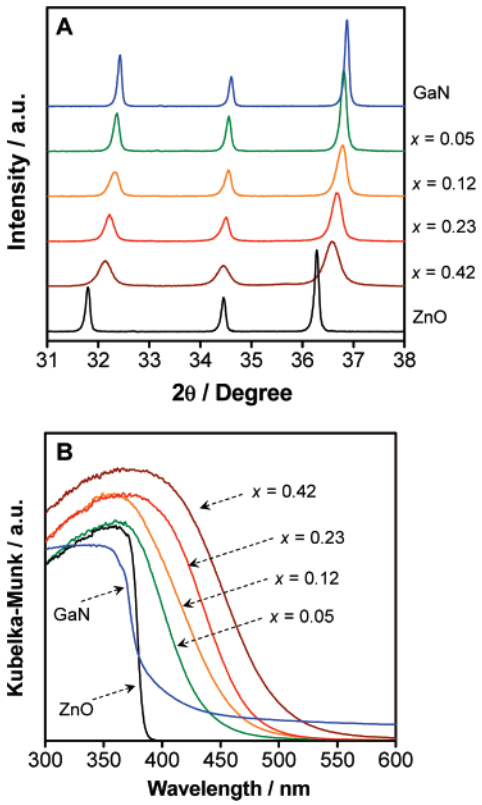

Figure 11. (A) Powder XRD patterns and (B) UV−visible diffuse reflectance spectra for various $(Ga_{1-x}Zn_x)(N_{1-x}O_x)$ solid solutions.

5.3. GaN−ZnO Solid Solution. To devise a new (oxy)nitride with d^{10} electronic configuration that can decompose water under visible light, the solid solution of GaN and ZnO, $(Ga_{1-x}Zn_x)$-$(N_{1-x}O_x)$, was examined. As both GaN and ZnO have wurtzite structures with similar lattice parameters,[77,78] a solid solution can be formed between the two. Taking into account the large band gap energies of GaN and ZnO (>3 eV), it had been considered that the band gap of the solid solution should exceed 3 eV. However, for II−VI semiconductors, it has been pointed out that p−d repulsion (e.g., O2p−Zn3d) shifts the valence band maximum upward without affecting the conduction band minimum.[79] Similarly, it was hypothesized that p−d repulsion in the GaN−ZnO solid solution (i.e., N2p−Zn3d repulsion) may cause the top of the valence band formed by N2p atomic orbitals to lift up to a higher potential energy, resulting in a narrower band gap for GaN.

The $(Ga_{1-x}Zn_x)(N_{1-x}O_x)$ solid solution is typically synthesized by nitriding a mixture of Ga_2O_3 and ZnO.[80,81] Elemental analyses by inductively coupled plasma optical emission spectroscopy (ICP−OES) have revealed that the ratios of Ga to N and Zn to

O in the as-prepared material are close to unity and that the N and O concentrations increase with the Ga and Zn concentrations, respectively.[80] The atomic composition of $(Ga_{1-x}Zn_x)(N_{1-x}O_x)$ is controllable by changing the nitridation conditions.[81] Figure 11A shows XRD patterns of samples with various compositions. All samples exhibit single-phase diffraction patterns indicative of the wurtzite structure similar to GaN and ZnO. The positions of the diffraction peaks are shifted successively to lower angles (2θ) with increasing Zn and O concentrations, indicating that the obtained samples are not physical mixtures of GaN and ZnO phases but rather solid solutions of GaN and ZnO. This peak shift is reasonable, as the lattice parameters of GaN are larger than those of ZnO (GaN: $a = b = 0.319$, $c = 0.519$ nm; ZnO: $a = b = 0.325$, $c = 0.521$ nm).[77,78] The same tendency has been confirmed by Rietveld analysis using the computer program RIETAN-2000, and neutron powder diffraction analysis has confirmed that the oxygen atom is substituted for the nitrogen atom in $(Ga_{1-x}Zn_x)(N_{1-x}O_x)$ with no interstitial site and no large disorder in the material.[82,83]

While GaN and ZnO both have band gap energies greater than 3 eV and thus do not absorb visible light, the $(Ga_{1-x}Zn_x)(N_{1-x}O_x)$ solid solution has absorption edges in the visible region. Figure 11B shows the UV−visible diffuse reflectance spectra for several samples. The absorption edge shifts to longer wavelengths with increasing Zn and O concentration (x) in $(Ga_{1-x}Zn_x)(N_{1-x}O_x)$. The band gap energies of the solid solutions are estimated to be 2.4−2.8 eV based on the diffuse reflectance spectra. As expected, DFT calculations indicate that the visible-light response of the solid solution originates from the contribution of Zn3d atomic orbitals to the valence band, where the bonding between Zn and N atoms is formed as a result of the formation of the solid solution.

The as-prepared $(Ga_{1-x}Zn_x)(N_{1-x}O_x)$ exhibits little photocatalytic activity for water decomposition even under UV irradiation. However, modification by surficial deposition of RuO_2 nanoparticles as H_2 evolution sites results in clearly observable H_2 and O_2 evolution. The photocatalytic activity increases remarkably with increasing RuO_2 content to a maximum at 5 wt % RuO_2, with the activity dropping gradually at higher RuO_2 loadings. It was elucidated by scanning electron microscopy (SEM), XPS, and X-ray absorption fine structure (XAFS) spectroscopy that the enhancement of photocatalytic activity by RuO_2 loading is related to the formation of crystalline RuO_2 nanoparticles with optimal particle size and coverage.[84] The photocatalytic performance of the RuO_2-loaded $(Ga_{1-x}Zn_x)(N_{1-x}O_x)$ is also dependent on both the pH of the aqueous solution[80] and the crystallinity and composition of $(Ga_{1-x}Zn_x)(N_{1-x}O_x)$.[81] The activity increases with decreasing pH from pH 7, reaching maximum activity at pH 3. Below pH 3, at which the activity begins to decrease, the surface of the catalyst is no longer completely stable due to the corrosion of surface Zn species. This tendency is similar to that observed for RuO_2-loaded β-Ge_3N_4.[76] The occurrence of peak activity in an acidic medium is consistent with the general characteristics of d^{10}-type (oxy)nitride materials, which are inherently unstable in basic media but stable in acidic media. Figure 12 shows a typical time course of overall water splitting on $(Ga_{1-x}Zn_x)(N_{1-x}O_x)$ ($x = 0.12$) loaded with 5 wt % RuO_2 under visible irradiation ($\lambda > 400$ nm). No reaction took place without irradiation, whereas both H_2 and O_2 evolved steadily and stoichiometrically upon irradiation in the visible region. Although it is known that O_2 evolution occurs on a ZnO electrode as a result of degradation when employed as a photoanode for water oxidation

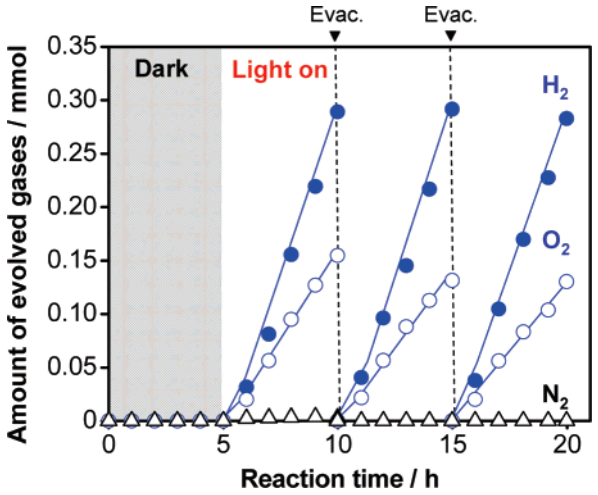

Figure 12. Typical time course of overall water splitting on 5 wt % RuO_2-loaded $(Ga_{1-x}Zn_x)(N_{1-x}O_x)$ ($x = 0.12$) under visible light ($\lambda > 400$ nm). Reaction conditions: 0.3 g of catalyst and 390 mL of distilled water; high-pressure mercury lamp light source (450 W); Pyrex inner irradiation-type reaction vessel with aqueous $NaNO_2$ filter.

in a photoelectrochemical cell,[85] it has been confirmed through ^{18}O-isotopic H_2O cleavage experiments that O_2 evolution on $(Ga_{1-x}Zn_x)(N_{1-x}O_x)$ is due to water oxidation, with the XRD pattern of the sample remaining unchanged after the reaction.[80] These results indicate that $(Ga_{1-x}Zn_x)(N_{1-x}O_x)$ functions as a stable visible-light-driven photocatalyst for overall water splitting. To the best of our knowledge, this is the first successful and reproducible example of overall water splitting by one-step photoexcitation using a particulate photocatalyst having a band gap in the visible region.

As shown in Figure 2, the photocatalytic activity of a given material is dependent on the cocatalyst, which plays the essential roles of inducing the photogeneration of carriers, constructing catalytic gas evolution sites, and reducing the activation energy required for gas evolution. A range of transition-metal oxides have been examined as cocatalysts to promote overall water splitting using $(Ga_{1-x}Zn_x)(N_{1-x}O_x)$, all of which are inactive for water formation from H_2 and O_2 and are thus well suited for overall water splitting. The cocatalysts are loaded by impregnation with the transition-metal precursors followed by calcination in air. Ni, Ru, Rh, Ir, and Pt oxides were found to be effective for promoting overall water splitting by $(Ga_{1-x}Zn_x)(N_{1-x}O_x)$ under UV irradiation. The activity of $(Ga_{1-x}Zn_x)(N_{1-x}O_x)$ modified with various transition-metal oxides as cocatalysts is further enhanced by coloading Cr oxide, although modification with Cr oxide alone is not effective for promoting activity in this reaction.[86,87] The activity of the coloaded catalyst is found to be strongly dependent on the amount of loaded Cr, which in turn varies according to the paired transition metal. The improvement in activity is attributed to the formation of suitable reaction sites by intimate interaction between Cr and the paired metal component.[87] Among the various materials examined, the largest improvement in activity was obtained when $(Ga_{1-x}Zn_x)(N_{1-x}O_x)$ was loaded with a mixed oxide of Rh and Cr. SEM, HR-TEM, EDX, XPS, and XAFS analyses confirmed that the loaded Rh and Cr species interact to form mixed-oxide ($Rh_{2-y}Cr_yO_3$) nanoparticles,10−30 nm in size with a trivalent electronic state.[88] The photocatalytic performance of the $Rh_{2-y}Cr_yO_3$-loaded $(Ga_{1-x}Zn_x)(N_{1-x}O_x)$ is strongly dependent on the pH of the reactant solution,[89] as in the case of RuO_2-loaded $(Ga_{1-x}Zn_x)(N_{1-x}O_x)$.[80] The photocatalyst exhibits stable and high photocatalytic activity in an aqueous solution at pH 4.5 for as long as 3 days. The photocatalytic performance at

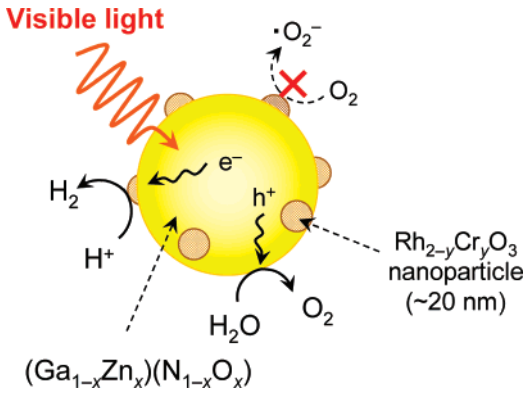

Figure 13. Schematic illustration of mechanism of visible-light-driven overall water splitting on $Rh_{2-y}Cr_yO_3$-loaded $(Ga_{1-x}Zn_x)(N_{1-x}O_x)$.

pH 3.0 and 6.2 is much lower, attributable to corrosion of the cocatalyst and hydrolysis of the catalyst. It has also been confirmed by XRD, XPS, and XAFS that the crystal structure of the catalyst and the valence state of both the surface and bulk do not change even after reaction for 3 days at optimal pH (4.5). The quantum efficiency of the $Rh_{2-y}Cr_yO_3$-loaded $(Ga_{1-x}Zn_x)(N_{1-x}O_x)$ catalyst for overall water splitting reaches ca. 2.5% at 420−440 nm, 10 times greater than that of the RuO_2-loaded catalyst (ca. 0.23%).[86] The improvement in activity achieved by loading the $(Ga_{1-x}Zn_x)(N_{1-x}O_x)$ catalyst with $Rh_{2-y}Cr_yO_3$ is attributable to promotion of the H_2 evolution reaction, which is the rate-determining step of overall water splitting, and inhibition of O_2 photoreduction.[89] A schematic illustration of the mechanism of overall water splitting on $Rh_{2-y}Cr_yO_3$-loaded $(Ga_{1-x}Zn_x)(N_{1-x}O_x)$ is shown in Figure 13. This $Rh_{2-y}Cr_yO_3$ cocatalyst is also applicable to other photocatalytic systems, such as TiO_2 and GaN, regardless of electronic configuration or the type of photocatalyst.[87,90]

5.4. $ZnGeN_2$−ZnO Solid Solution. A solid solution of $ZnGeN_2$ and ZnO, $(Zn_{1+x}Ge)(N_2O_x)$, has also been found to be an active and stable photocatalyst for overall water splitting under visible light.[91] $ZnGeN_2$ forms a hexagonal monoclinic phase with similar lattice parameters to ZnO, constituting a hexagonal wurtzite structure.[92] Both $ZnGeN_2$ and ZnO are wide-gap semiconductors with band gaps larger than 3 eV, although the band gap of $ZnGeN_2$ is dependent on the crystal structure and composition.[93] Nitridation of ZnO and GeO_2 (Zn/Ge = 5 by mole) at 1123 K for 15 h under a flow of NH_3 (20 mL/min) results in a pale-yellow powder with an atomic composition of $(Zn_{1.44}Ge)(N_{2.08}O_{0.38})$. The crystal structure of the material was confirmed by Rietveld analysis and neutron powder diffraction to be wurtzite with space group $P6_3mc$. In the solid solution between $ZnGeN_2$ and ZnO, the oxygen atoms are replaced with nitrogen sites. The band gap of the material is estimated to be ca. 2.7 eV based on the absorption edges, which is smaller than the band gaps of β-Ge_3N_4 (ca. 3.8 eV), $ZnGeN_2$ (ca. 3.3 eV), and ZnO (ca. 3.2 eV). The visible-light response of the material originates from the wide valence bands consisting of N2p, O2p, and Zn3d atomic orbitals and p−d repulsion between Zn3d and N2p + O2p electrons in the upper part of the valence bands.

Neither $ZnGeN_2$ nor ZnO alone exhibit photocatalytic activity for overall water splitting under UV irradiation. However, the solid solution $(Zn_{1.44}Ge)(N_{2.08}O_{0.38})$ becomes photocatalytically active under UV and visible irradiation when loaded with nanoparticulate RuO_2. Overall water splitting on RuO_2-loaded $(Zn_{1.44}Ge)(N_{2.08}O_{0.38})$ proceeds by band gap photoexcitation from the valence band formed by N2p, O2p, and Zn3d atomic orbitals to the conduction band consisting of Ge4s,4p hybridized atomic orbitals, without noticeable degradation.

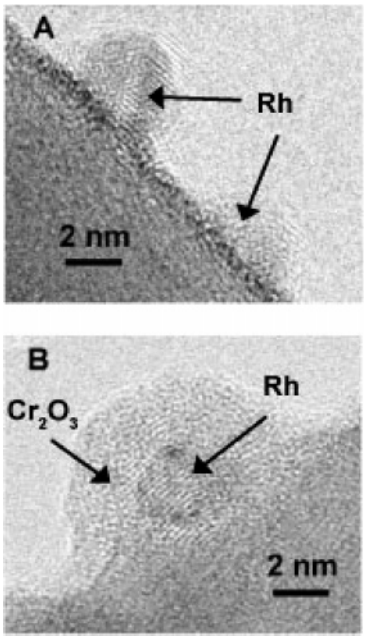

Figure 14. HR-TEM images of $(Ga_{1-x}Zn_x)(N_{1-x}O_x)$ ($x = 0.12$) with photodeposited Rh (A) before and (B) after further photodeposition of a Cr_2O_3 shell.

6. Noble Metal/Cr_2O_3 (Core/Shell) Nanoparticle as a New Type of Cocatalyst

(Oxy)nitrides exhibit relatively high photocatalytic activity for water oxidation in the presence of an appropriate electron acceptor.[55−58,86] However, the activity for water reduction is approximately 1 order of magnitude lower than that for water oxidation. The overall efficiency of these (oxy)nitride-based catalysts can thus be improved by modification to promote water reduction. The most conventional modification of a photocatalyst to improve water reduction is loading a cocatalyst by impregnation. This approach produces a random dispersion of active species on the photocatalyst surface, and activation treatment, such as reduction or oxidation, is necessary to obtain high activity.[5,7,9−22,24−30,74−76,80,81,84,86−91] Activation treatment is inherently unsuitable for (oxy)nitrides, which are less thermally stable than the corresponding metal oxides.[94] In contrast, in situ photodeposition allows the cocatalyst to be loaded selectively at reaction sites and does not require subsequent activation treatment.[95] However, most of the cocatalysts suitable for introduction by this method are noble metals (e.g., Rh, Pd, and Pt), which act as a catalyst not only for water reduction but also for water formation from H_2 and O_2, an undesirable backward reaction.[6] A new modification method that achieves the introduction of a water-reducing cocatalyst without the need for activation treatment is therefore desired.

A new type of H_2 evolution cocatalyst was thus developed, a noble metal/Cr_2O_3 (core/shell) nanoparticulate cocatalysts that can be prepared by in situ photodeposition.[96] Figure 14 shows HR-TEM images of Rh-loaded $(Ga_{1-x}Zn_x)(N_{1-x}O_x)$ ($x = 0.12$) before and after photodeposition of the Cr_2O_3 shell. In this system, the Rh nanoparticles forming the core induce the migration of photogenerated electrons from the $(Ga_{1-x}Zn_x)(N_{1-x}O_x)$ bulk to the surface, while the Cr_2O_3 shell provides a H_2 evolution site at the external surface and simultaneously inhibits water formation from H_2 and O_2 on Rh. In photocatalytic overall water

splitting, cocatalysts such as NiO_x, RuO_2, and $Rh_{2-y}Cr_yO_3$ play at least two roles simultaneously, that is, extraction of photogenerated electrons from the photocatalyst bulk and reduction of H^+ to H_2 on the cocatalyst surface. In contrast, these two roles are successfully separated in the new core/shell cocatalyst system, which will also be of interest in the study of the respective roles of cocatalytic components.

One of the present authors has also reported Ni-core/NiO-shell nanoparticles as another core/shell cocatalyst for photocatalytic overall water splitting,[5,9] and this cocatalysts has been applied to many heterogeneous photocatalytic systems.[5,9,11,14,15,17,21,87] Compared with Ni/NiO, the noble metal/Cr_2O_3 core/shell cocatalyst has several advantages, including the possibility of selective introduction of active species for overall water splitting at reduction sites of the photocatalyst, the possibility of using various noble and transition metals as a core for extraction of photogenerated electrons from the bulk, and elimination of the need for activation treatment by oxidation or reduction. The noble metal/Cr_2O_3 modification method, therefore, provides a new strategy for the construction of water-reducing cocatalysts for photocatalytic overall water splitting.

7. Summary and Outlook

A range of non-oxide materials for photocatalytic overall water splitting have been developed by the authors' group. (Oxy)nitrides and oxysulfides have been found to function as stable photocatalysts for water reduction and oxidation under visible irradiation, and the $(Ga_{1-x}Zn_x)(N_{1-x}O_x)$ and $(Zn_{1+x}Ge)$-(N_2O_x) solid solutions have been shown to achieve overall water splitting under visible light without noticeable degradation. As all of the successful photocatalysts developed for overall water splitting in the past 30 years are comprised solely of metal oxides and are largely ineffective under visible light, the discovery of non-oxide photocatalysts achieving the same function is expected to reinvigorate research on photocatalysts for solar energy conversion.

Our group has suggested that a tentative goal for research on hydrogen production via solar-driven overall water splitting using a particulate photocatalyst is to develop a stable material that can achieve quantum efficiency of 30% at 600 nm. If such a photocatalytic system can be successfully constructed, the solar-to-hydrogen energy conversion efficiency is estimated to be ca. 5%, which is still lower than that achieved by PEC cells. Nevertheless, such a goal is considered to be a good starting point for practical application, given the simple and scalable nature of this approach. The state of the art in this field is, at most, quantum efficiency of a few percent at wavelengths as long as 500 nm. Therefore, more efficient photocatalytic materials with a band gap as narrow as 2 eV (corresponding to 600 nm) will need to be developed. At the same time, the reaction kinetics in photocatalysis should be investigated as a means of refining the materials to maximize efficiency and optimize preparation.

Acknowledgment. The research described herein was supported by the Core Research for Evolutional Science and Technology (CREST) and Solution Oriented Research for Science and Technology (SORST) programs of the Japan Science and Technology Corporation (JST). Acknowledgment is also extended to the 21st Century Center of Excellence (COE) and the Research and Development in a New Interdisciplinary Field Based on Nanotechnology and Materials Science programs of the Ministry of Education, Culture, Sports, Science and Technology (MEXT) of Japan.

References and Notes

(1) Fujishima, A.; Honda, K. *Nature* **1972**, *238*, 37−38.
(2) Sakai, Y.; Sugahara, S.; Matsumura, M.; Nakato, Y.; Tsubomura, H. *Can. J. Chem.* **1988**, *66*, 1853−1856.
(3) Khaselev, O.; Turner, J. A. *Science* **1998**, *280*, 425−427.
(4) Licht, S.; Wang, B.; Mukerji, S.; Soga, T.; Umeno, M.; Tributsch, H. *J. Phys. Chem. B* **2000**, *104*, 8920−8924.
(5) Domen, K.; Naito, S.; Soma, M.; Onishi, T.; Tamaru, K. *J. Chem. Soc., Chem. Commun.* **1980**, 543−544.
(6) Sato, S.; White, J. M. *Chem. Phys. Lett.* **1980**, *72*, 83−86.
(7) Lehn, J. M.; Sauvage, J. P.; Ziessel, R. *Nouv. J. Chim.* **1980**, *4*, 623−627.
(8) Bard, A. J.; Fox, M. A. *Acc. Chem. Res.* **1995**, *28*, 141−145.
(9) Domen, K.; Naito, S.; Onishi, T.; Tamaru, K. *Chem. Phys. Lett.* **1982**, *92*, 433−434.
(10) Domen, K.; Kudo, A.; Shinozaki, A.; Tanaka, A.; Maruya, K.; Onishi, T. *J. Chem. Soc., Chem. Commun.* **1986**, 356−357.
(11) Kudo, A.; Tanaka, A.; Domen, K.; Maruya, K.; Aika, K.; Onishi, T. *J. Catal.* **1988**, *111*, 67−76.
(12) Inoue, Y.; Kubokawa, T.; Sato, K. *J. Chem. Soc., Chem. Commun.* **1990**, 1298−1299.
(13) Inoue, Y.; Niiyama, T.; Asai, Y.; Sato, K. *J. Chem. Soc., Chem. Commun.* **1992**, 579−580.
(14) Takata, T.; Furumi, Y.; Shinohara, K.; Tanaka, A.; Hara, M.; Kondo, J. N.; Domen, K. *Chem. Mater.* **1997**, *9*, 1063−1064.
(15) Ikeda, S.; Hara, M.; Kondo, J. N.; Domen, K.; Takahashi, H.; Okubo, T.; Kakihana, M. *J. Mater. Res.* **1998**, *13*, 852−855.
(16) Kudo, A.; Kato, H. *Chem. Lett.* **1997**, *26*, 867−877.
(17) Kim, H. G.; Hwang, D. W.; Kim, J.; Kim, Y. G.; Lee, J. S. *Chem. Commun.* **1999**, 1077−1078.
(18) Kato, H.; Kudo, A. *Chem. Phys. Lett.* **1998**, *295*, 487−492.
(19) Machida, M.; Yabunaka, J.; Kijima, T. *Chem. Commun.* **1999**, 1939−1940.
(20) Kato, H.; Kudo, A. *J. Phys. Chem. B* **2001**, *105*, 4285−4292.
(21) Shimizu, K.; Tsuji, Y.; Kawakami, M.; Toda, K.; Kodama, T.; Sato, M.; Kitayama, Y. *Chem. Lett.* **2002**, *31*, 1158−1159.
(22) Kato, H.; Asakura, K.; Kudo, A. *J. Am. Chem. Soc.* **2003**, *125*, 3082−3089.
(23) Sayama, K.; Arakawa, H. *J. Phys. Chem.* **1993**, *97*, 531−533.
(24) Ikeda, S.; Itani, T.; Nango, K.; Matsumura, M. *Catal. Lett.* **2004**, *98*, 229−233.
(25) Sato, J.; Saito, N.; Nishiyama, H.; Inoue, Y. *J. Phys. Chem. B* **2001**, *105*, 6061−6063.
(26) Ikarashi, K.; Sato, J.; Kobayashi, H.; Saito, N.; Nishiyama, H.; Inoue, Y. *J. Phys. Chem. B* **2002**, *106*, 9048−9053.
(27) Sato, J.; Saito, N.; Nishiyama, H.; Inoue, Y. *J. Photochem. Photobiol., A* **2002**, *148*, 85−89.
(28) Sato, J.; Kobayashi, H.; Saito, N.; Nishiyama, H.; Inoue, Y. *J. Photochem. Photobiol., A* **2003**, *158*, 139−144.
(29) Sato, J.; Saito, N.; Nishiyama, H.; Inoue, Y. *J. Phys. Chem. B* **2003**, *107*, 7965−7969.
(30) Sato, J.; Kobayashi, H.; Ikarashi, K.; Saito, N.; Nishiyama, H.; Inoue, Y. *J. Phys. Chem. B* **2004**, *108*, 4369−4375.
(31) Scaife, D. E. *Sol. Energy* **1980**, *25*, 41−54.
(32) Matsumura, M.; Saho, Y.; Tsubomura, H. *J. Phys. Chem.* **1983**, *87*, 3807−3808.
(33) Reber, J. F.; Meier, K. *J. Phys. Chem.* **1986**, *90*, 824−834.
(34) Krasnovsky, A. A.; Brin, G. P. *Dokl. Akad. Nauk.* **1962**, *147*, 656−659.
(35) Darwent, J. R.; Mills, A. *J. Chem. Soc., Faraday Trans. 2* **1982**, *78*, 359−367.
(36) Erbs, W.; Desilvestro, J.; Borgarello, E.; Grätzel, M. *J. Phys. Chem.* **1984**, *88*, 4001−4006.
(37) Williams, R. *J. Chem. Phys.* **1960**, *32*, 1505−1514.
(38) Ellis, A. B.; Kaiser, S. W.; Bolts, J. M.; Wrighton, M. S. *J. Am. Chem. Soc.* **1977**, *99*, 2839−2848.
(39) Yoshimura, J.; Ebina, Y.; Kondo, J.; Domen, K.; Tanaka, A. *J. Phys. Chem.* **1993**, *97*, 1970−1973.
(40) Kudo, A.; Mikami, I. *Chem. Lett.* **1998**, *27*, 1027−1028.
(41) Kudo, A.; Ueda, K.; Kato, H.; Mikami, I. *Catal. Lett.* **1998**, *53*, 229−230.
(42) Kudo, A.; Omori, K.; Kato, H. *J. Am. Chem. Soc.* **1999**, *121*, 11459−11467.
(43) Sayama, K.; Mukasa, K.; Abe, R.; Abe, Y.; Arakawa, H. *Chem. Commun.* **2001**, 2416−2417.
(44) Kato, H.; Kudo, A. *J. Phys. Chem. B* **2002**, *106*, 5029−5034.
(45) Kato, H.; Kobayashi, H.; Kudo, A. *J. Phys. Chem. B* **2002**, *106*, 12441−12447.
(46) Hosogi, Y.; Tanabe, K.; Kato, H.; Kobayashi, H.; Kudo, A. *Chem. Lett.* **2004**, *33*, 28−29.
(47) Konta, R.; Ishii, T.; Kato, H.; Kudo, A. *J. Phys. Chem. B* **2004**, *108*, 8992−8995.

(48) Kim, H. G.; Hwang, D. W.; Lee, J. S. *J. Am. Chem. Soc.* **2004**, *126*, 8912−8913.
(49) Kato, H.; Hori, M.; Konta, R.; Shimodaira, Y.; Kudo, A. *Chem. Lett.* **2004**, *33*, 1348−1349.
(50) Hwang, D. W.; Kim, H. G.; Lee, J. S.; Kim, J.; Li, W.; Oh, S. H. *J. Phys. Chem. B* **2005**, *109*, 2093−2102.
(51) Kim, H. G.; Borse, P. H.; Choi, W.; Lee, J. S. *Angew. Chem., Int. Ed.* **2005**, *44*, 4585−4589.
(52) Abe, R.; Sayama, K.; Sugihara, H. *J. Phys. Chem. B* **2005**, *109*, 16052−16061.
(53) Asahi, R.; Morikawa, T.; Ohwaki, T.; Aoki, K.; Taga, Y. *Science* **2001**, *293*, 269−271.
(54) Jansen, M.; Letschert, H. P. *Nature* **2000**, *404*, 980−982.
(55) Hitoki, G.; Takata, T.; Kondo, J. N.; Hara, M.; Kobayashi, H.; Domen, K. *Chem. Commun.* **2002**, 1698−1699.
(56) Hitoki, G.; Ishikawa, A.; Takata, T.; Kondo, J. N.; Hara, M.; Domen, K. *Chem. Lett.* **2002**, *31*, 736−737.
(57) Hitoki, G.; Takata, T.; Kondo, J. N.; Hara, M.; Kobayashi, H.; Domen, K. *Electrochemistry (Tokyo, Jpn.)* **2002**, *70*, 463−465.
(58) Kasahara, A.; Nukumizu, K.; Hitoki, G.; Takata, T.; Kondo, J. N.; Hara, M.; Kobayashi, H.; Domen, K. *J. Phys. Chem. A* **2002**, *106*, 6750−6753.
(59) Kasahara, A.; Nukumizu, K.; Takata, T.; Kondo, J. N.; Hara, M.; Kobayashi, H.; Domen, K. *J. Phys. Chem. B* **2003**, *107*, 791−797.
(60) Nukumizu, K.; Nunoshige, J.; Takata, T.; Kondo, J. N.; Hara, M.; Kobayashi, H.; Domen, K. *Chem. Lett.* **2003**, *32*, 196−197.
(61) Hara, M.; Chiba, E.; Ishikawa, A.; Takata, T.; Kondo, J. N.; Domen, K. *J. Phys. Chem. B* **2003**, *107*, 13441−13445.
(62) Yamasita, D.; Takata, T.; Hara, M.; Kondo, J. N.; Domen, K. *Solid State Ionics* **2004**, *172*, 591−595.
(63) Chun, W. A.; Ishikawa, A.; Fujisawa, H.; Takata, T.; Kondo, J. N.; Hara, M.; Kawai, M.; Matsumoto, Y.; Domen, K. *J. Phys. Chem. B* **2003**, *107*, 1798−1803.
(64) Lu, D.; Hitoki, G.; Katou, E.; Kondo, J. N.; Hara, M.; Domen, K. *Chem. Mater.* **2004**, *16*, 1603−1605.
(65) Hara, M.; Nunoshige, J.; Takata, T.; Kondo, J. N.; Domen, K. *Chem. Commun.* **2003**, 3000−3001.
(66) Lee, Y.; Nukumizu, K.; Watanabe, T.; Takata, T.; Hara, M.; Yoshimura, M.; Domen, K. *Chem. Lett.* **2006**, *35*, 352−353.
(67) Ishikawa, A.; Takata, T.; Kondo, J. N.; Hara, M.; Domen, K. *J. Phys. Chem. B* **2004**, *108*, 11049−11053.
(68) Abe, R.; Takata, T.; Sugihara, H.; Domen, K. *Chem. Commun.* **2005**, 3829−3830.
(69) Ishikawa, A.; Takata, T.; Kondo, J. N.; Hara, M.; Kobayashi, H.; Domen, K. *J. Am. Chem. Soc.* **2002**, *124*, 13547−13553.
(70) Ishikawa, A.; Yamada, Y.; Takata, T.; Kondo, J. N.; Hara, M.; Kobayashi, H.; Domen, K. *Chem. Mater.* **2003**, *15*, 4442−4446.
(71) Ishikawa, A.; Takata, T.; Matsumura, T.; Kondo, J. N.; Hara, M.; Kobayashi, H.; Domen, K. *J. Phys. Chem. B* **2004**, *108*, 2637−2642.
(72) Harriman, A.; Thomas, J. M.; Millward, G. R. *New J. Chem.* **1987**, *11*, 757−762.
(73) Harriman, A.; Pickering, I. J.; Thomas, J. M.; Christensen, P. A. *J. Chem. Soc., Faraday Trans. 1* **1988**, *84*, 2795−2806.
(74) Sato, J.; Saito, N.; Yamada, Y.; Maeda, K.; Takata, T.; Kondo, J. N.; Hara, M.; Kobayashi, H.; Domen, K.; Inoue, Y. *J. Am. Chem. Soc.* **2005**, *127*, 4150−4151.
(75) Lee, Y.; Watanabe, T.; Takata, T.; Hara, M.; Yoshimura, M.; Domen, K. *J. Phys. Chem. B* **2006**, *110*, 17563−17569.
(76) Maeda, K.; Saito, N.; Lu, D.; Inoue, Y.; Domen, K. *J. Phys. Chem. C* **2007**, *111*, 4749−4755.
(77) Suhulz, H.; Thiemann, K. H. *Solid State Commun.* **1977**, *23*, 815−819.
(78) Garcia-Martinez, O.; Rojas, R. M.; Vila, E.; Martin de Vidales, J. L.; *Solid State Ionics* **1997**, *63*, 442−449.
(79) Wei, S. H.; Zunger, A. *Phys. Rev. B* **1988**, *37*, 8958−8981.
(80) Maeda, K.; Takata, T.; Hara, M.; Saito, N.; Inoue, Y.; Kobayashi, H.; Domen, K. *J. Am. Chem. Soc.* **2005**, *127*, 8286−8287.
(81) Maeda, K.; Teramura, K.; Takata, T.; Hara, M.; Saito, N.; Toda, K.; Inoue, Y.; Kobayashi, H.; Domen, K. *J. Phys. Chem. B* **2005**, *109*, 20504−20510.
(82) Yashima, M.; Maeda, K.; Teramura, K.; Takata, T.; Domen, K. *Chem. Phys. Lett.* **2005**, *416*, 225−227.
(83) Yashima, M.; Maeda, K.; Teramura, K.; Takata, T.; Domen, K. *Mater. Trans.* **2006**, *47*, 295−297.
(84) Teramura, K.; Maeda, K.; Saito, T.; Takata, T.; Saito, N.; Inoue, Y.; Domen, K. *J. Phys. Chem. B* **2005**, *109*, 21915−21921.
(85) Gerischer, H. *J. Electrochem. Soc.* **1966**, *113*, 1174−1182.
(86) Maeda, K.; Teramura, K.; Lu, D.; Takata, T.; Saito, N.; Inoue, Y.; Domen, K. *Nature* **2006**, *440*, 295.
(87) Maeda, K.; Teramura, K.; Saito, N.; Inoue, Y.; Domen, K. *J. Catal.* **2006**, *243*, 303−308.
(88) Maeda, K.; Teramura, K.; Lu, D.; Takata, T.; Saito, N.; Inoue, Y.; Domen, K. *J. Phys. Chem. B* **2006**, *110*, 13753−13758.
(89) Maeda, K.; Teramura, K.; Masuda, H.; Takata, T.; Saito, N.; Inoue, Y.; Domen, K. *J. Phys. Chem. B* **2006**, *110*, 13107−13112.
(90) Maeda, K.; Teramura, K.; Saito, N.; Inoue, Y.; Domen, K. *Bull. Chem. Soc. Jpn.* **2007**, in press.
(91) Lee, Y.; Terashima, H.; Shimodaira, Y.; Teramura, K.; Hara, M.; Kobayashi, H.; Domen, K.; Yashima, M. *J. Phys. Chem. C* **2007**, *111*, 1042−1048.
(92) Larson, W. L.; Maruska, H. P.; Stevenson, D. A. *J. Electrochem. Soc.* **1974**, *121*, 1673−1674.
(93) Misaki, T.; Wu, X.; Wakahara, A.; Yoshida, A. *Proc. Int. Workshop Nitride Semicond.* **2000**, *1*, 685−688.
(94) Le Gendre, L.; Marchand, R.; Laurent, Y. *J. Eur. Ceram. Soc.* **1997**, *17*, 1813−1818.
(95) Kraeutler, B.; Bard, A. J. *J. Am. Chem. Soc.* **1978**, *100*, 4317−4318.
(96) Maeda, K.; Teramura, K.; Lu, D.; Saito, N.; Inoue, Y.; Domen, K. *Angew. Chem., Int. Ed.* **2006**, *45*, 7806−7809.